PCCP

COMMUNICATION

View Article Online
View Journal | View Issue

Cite this: *Phys. Chem. Chem. Phys.*, 2017, **19**, 12633

Received 23rd March 2017,
Accepted 18th April 2017

DOI: 10.1039/c7cp01870c

rsc.li/pccp

The shielding cone in spherical aromatic structures: insights from models for spherical $2(N + 1)^2$ aromatic fullerenes†

Alvaro Muñoz-Castro [ab]

A direct correlation between π- and spherical aromaticity of the aromatic structures was established by showing that they shared a characteristic shielding cone, resulting from a specific orientation of the applied field. Herein, we revealed the presence of a related long-range shielding cone in spherical aromatic species that was demonstrated through C_{20}, C_{32}, C_{50}, and C_{60} Hirsh aromatic fullerenes. It was found that while for planar aromatics, the cone is reserved only for a perpendicularly applied field, for spherical aromatic compounds, the three-dimensional cage allows the formation of a shielding cone according to the given orientation of the external field.

Since Kekulés seminal work on the rationalization of the benzene structure, involving conjugated single and double bonds within the ring,[1–3] aromatic molecules continue to attract the interest from the scientific community.[4–12] An indubitable characteristic of these systems is their capacity to exhibit a free π-electron precession under an external applied magnetic field. This current circulation of electrons builds up an induced magnetic field, opposing or shielding the external field at the center of the ring, being complemented by a deshielding region at the outer contour, rationalized through the early Pople ring current model.[13] This resulting shielding cone[6,14–18] exhibits a long-range behavior, leading to changes in the nuclear shielding of neighboring molecules, as observed from regular NMR experiments.[19–21]

A relevant extension of the concept of aromaticity is the realization of three-dimensional aromatic systems, involving a spherical aromatic behavior. The Hirsch $2(N + 1)^2$ electron count is particularly useful in determining the electronic structure requirements, in analogy to the Huckel $(4n + 2)\pi$ rule, widely employed for planar structures. The fascinating spherical structure of buckminsterfullerene (C_{60}),[22] is the prototypical example of a potential spherical aromatic structure.[23] However, its aromatic character has been the focus of controversy,[24] where a non-aromatic character appears as a more appropriate definition, due to the fact that C_{60} with 60 π-electrons does not satisfy the Hirsch rule.[25–31]

A truly aromatic counterpart is given by the hypothetical C_{60}^{10+}, depicting a 50 π-electron system ($N = 4$).[27,32,33] This favors electron delocalization and thus bond equalization. In consequence, the endohedral shielding is drastically enhanced from −2.8 ppm for C_{60} to −81.4 ppm for C_{60}^{10+} at the origin of the structure,[34] as expected for spherical aromatic species.[9] Generally, the description of the spherical aromatic behavior by the magnetic criteria[9] is based on the response inside the cage structure, in connection to the studies of planar aromatics. Herein, we went one step further by accounting for the response at the surroundings of the cage, which has been studied to a lesser extent. In this context, we explored the behavior of models for spherical aromatic fullerenes when they are exposed to a certain orientation of the applied field, based on 18-, 32-, and 50-π electron fullerenes ($N = 2$, 3 and 4), ranging from the smaller cage to the C_{60} cage, represented by C_{20}^{2+}, C_{32}, C_{50}, and C_{60}^{10+}.

Geometry optimizations and subsequent calculations were performed using DFT methods, employing the ADF 2016 code[35] with an all-electron triple-ξ Slater basis set plus the double-polarization (STO-TZ2P) basis set in conjunction with the Becke–Perdew (BP86) functional within the generalized gradient approximation (GGA).[36,37] The nuclear and nucleus-independent shielding tensors[6,14,38] were calculated within the GIAO formalism, employing the Perdew, Burke, and Ernzerhof[39,40] GGA exchange expression and all-electron STO-TZ2P basis set. To evaluate the magnetic response or induced field (B^{ind}) upon an external magnetic field (B^{ext}) at the molecular surroundings, a map representation of the nucleus-independent shielding tensor (σ_{ij}) was obtained, where $B_i^{ind} = -\sigma_{ij}B_j^{ext}$.[6,14,41–43] For convenience, the i and j suffixes were related to the x-, y-, and z-axes of the molecule-fixed Cartesian system ($i, j = x, y, z$). B^{ind} is given in ppm in relation to B^{ext}.

In Fig. 1, the orientational-averaged magnetic (isotropic) response for C_{60}, given by $B_{iso}^{ind} = -(1/3)(\sigma_{xx} + \sigma_{yy} + \sigma_{zz})B_j^{ext}$, is

[a] *Grupo de Química Inorgánica y Materiales Moleculares, Universidad Autonoma de Chile, El Llano Subercaseaux 2801, Santiago, Chile. E-mail: alvaro.munoz@uautonoma.cl*

[b] *Relativistic Molecular Physics (ReMoPh) Group, Universidad Andres Bello, Republica 275, Santiago, Chile*

† Electronic supplementary information (ESI) available: Induced magnetic field of C_{60}^{10+} under different orientation of the applied field. See DOI: 10.1039/c7cp01870c

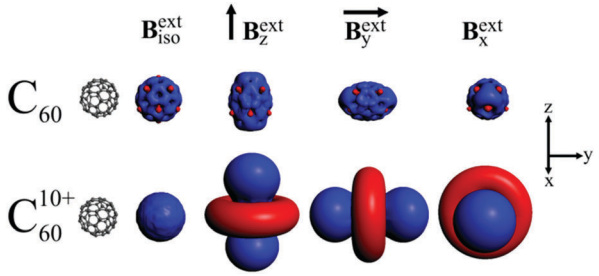

Fig. 1 Three-dimensional representation of the magnetic response (induced magnetic field, B^{ind}) for C_{60} and C_{60}^{10+}, in relation to the orientational-averaged (iso), and certain orientations of the applied field (B_i^{ext}, $i = x, y,$ and z). Isosurface values set at 2 ppm relative to the external field. Shielding, Blue/Deshielding, Red.

similar to that observed by Kleinpeter *et al.*,[44] denoting an alternate shielding/deshielding short range response at the six and five-membered rings, respectively. For certain orientations of the applied field, a similar response was found, denoting the short-range or local character of the response, which remains close to the C_{60} backbone.[34] This is due to the diminished response[33] for the 60-π electron system in comparison to the related Hirsch aromatic counterpart. In contrast, B_{iso}^{ind} for C_{60}^{10+} exhibits a shielding response in both six and five-membered rings, leading to a shielding sphere. Under a specific orientation of the applied field, the complexity of the overall magnetic behavior of fullerene can be unraveled, from which a long-range shielding response parallel to the applied field was found, with a complementary deshielding region contained in the perpendicular plane.

Interestingly, from the three-dimensional representation of B_i^{ind} ($I = x$-, y-, and z-axis), the shielding response when exposed to a certain orientation of the field, nicely resembles the long-range shielding cone widely discussed in planar aromatic rings.[6,24,25,31–33] Moreover, the complementary deshielding region is always located in a perpendicular plane in relation to the external field. This observation allows a direct correlation between the shielding cone of benzene and that obtained in C_{60}^{10+} (Fig. 2). Thus, another connection between planar and spherical aromatic compounds is revealed,[45] due to the formation of a long range shielding cone in both structures.

Note that for the smaller fullerene cage fulfilling the Hirsh rule, namely C_{20}^{2+}, the same behavior was observed (Fig. 3). The orientational-averaged magnetic response is similar to that of C_{60}^{10+}, which also exhibits an overall shielding response. From the specific orientation of the applied field, a shielding cone was also obtained, revealing a strong similarly between the 18- and 50-π electron Hirsh aromatic fullerenes.

The next spherical aromatic fullerene expected from the $2(N + 1)^2$ rule when $N = 3$ is given by the neutral form of C_{32}. For this structure, two low-lying isomers were depicted with a near spherical cage, namely D_3- and D_4-C_{32}, according to the respective point group. Our calculation suggests a separation of 5.6 kcal mol^{-1}, favoring the D_4 isomer, in agreement with previous reports.[46,47] Contrary to D_4-C_{32}, D_3-C_{32} exhibits five- and six-membered rings, involving an additional four-membered face, denoting structural differences between these isomers. Both C_{32} isomers show a similar behavior as observed for 18- and 50-π electron fullerenes, with an overall shielding response for the orientational-averaged magnetic response and a shielding cone for the specific orientation of the external field (Fig. 3).

Another example of a 50-π electron fullerene is given by the neutral C_{50} where two low-lying isomers, namely D_3- and D_{5h}-C_{50}, has been ascribed to the ground state.[48,49] The D_3 isomer is more stable, depicting a near spherical cage, in contrast to the D_{5h}-C_{50}, featuring an oblate structure. From earlier reports, following the characterization of the first fullerene derivative,[50] D_3-C_{50} has been depicted as highly aromatic and D_{5h}-C_{50} as non-aromatic. Recently, this spherical aromatic character has been revisited,[51] pointing out the importance of exhibiting a spherical shape. By comparing both isomers, the orientational-averaged magnetic response for the former is similar to that for the Hirsch aromatic fullerenes discussed above, depicting a shielding response as a spherical region. However, for D_{5h}-C_{50}, both short-ranged shielding and deshielding regions originate. This behavior resembles that of buckminsterfullerene (C_{60}), where deshielding zones are located over the five-membered rings and shielding zones are located at the six-membered rings, denoting the local nature of the response. This supports the non-aromatic character of C_{50}, which is similar to that of C_{60} (Fig. 1 and 3).

When the field is applied from certain orientations, D_3-C_{50} nicely resembles the behavior observed for 18-, 32-, and 50-π

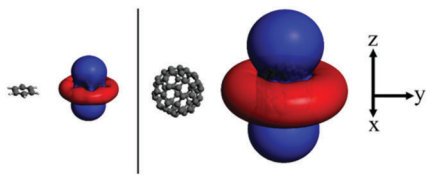

Fig. 2 Comparison of the induced shielding cone of benzene (left) and C_{60}^{10+} (right) under an external field oriented along the z-axis. Isosurface values set at 2 ppm relative to the external field. Shielding, Blue/Deshielding, Red.

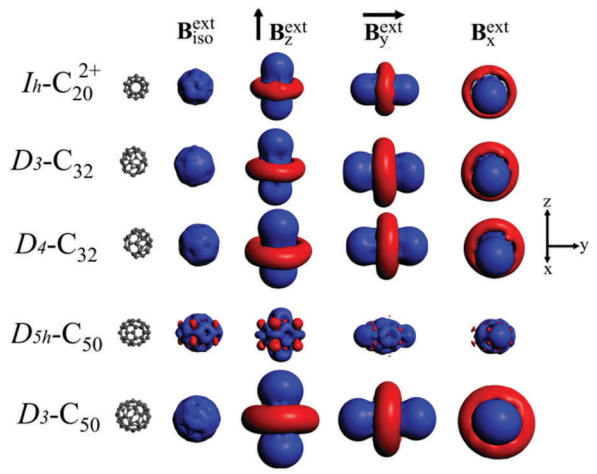

Fig. 3 Three-dimensional representation of the magnetic response B^{ind} for different fullerenes, in relation to the orientational-averaged external field (B_{iso}^{ext}), and a specific orientation of the applied field (B_z^{ext}). Isosurface values set at 2 ppm relative to the external field.

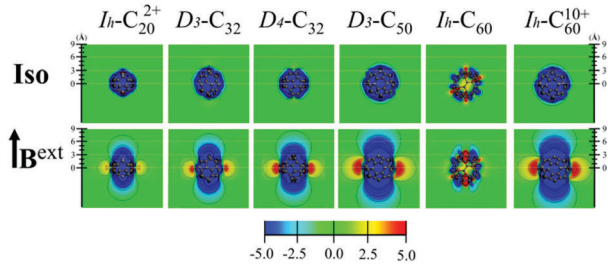

Fig. 4 Contour plot representation of the magnetic response B^{ind} for different fullerenes, in relation to the orientational-averaged external field (B_{iso}^{ext}), and a specific orientation of the applied field (B_z^{ext}). Color code from −5 to +5 ppm relative to the external field.

spherical fullerenes, where a long-range shielding cone response is originated parallel to the external field. In contrast, D_{5h}-C_{50} exhibits a short-range response, as observed for I_h-C_{60}, owing to its non-aromatic character.[33]

A comparison of the response between different fullerenes studied is given in Fig. 4. Interestingly, for the non-aromatic C_{60}, the response under a specific orientation of the external field and the orientational-averaged response are similar, denoting the short-range character of the response dominated by the antiaromatic character of the five-membered rings.[33] In contrast, for the Hirsh aromatic fullerenes, the isotropic response is similar along the series, in which under a specific orientation, the characteristic long-range shielding cone from planar aromatic compounds is recovered (see above). In this sense, for C_{20}^{2+}, the shielding region of the shielding cone amounting to −5 ppm is located at 4.6 Å from the center, and that of −2 ppm is located at 6.0 Å. For both C_{32} isomers, the region of −5 and −2 ppm are located at 4.7 and 7.8 Å, which increases to 7.3 and 10.0 Å in the D_3-C_{50} structure. In C_{60}^{10+}, the shielding cone with −5 ppm is located at 8.9 Å from the center and that with −2 ppm is located at 12.5 Å. This demonstrates the long-range character of the obtained shielding cone in spherical aromatic compounds. In benzene, the shielding cone exhibits these values at 3.6 and 5.2 Å.

As a result, planar and three-dimensional aromatic compounds share an inherent characteristic provided by the shielding cone, resulting from a specific orientation of the applied field. Interestingly, for planar aromatics, this property is reserved only for a perpendicularly applied field, whereas for spherical aromatic compounds, the three-dimensional cage allows the formation of the shielding cone according to the given orientation of the external field. Several orientations of B^{ext} were tested for C_{60}^{10+} (Fig. S1, ESI†), and the findings supported the abovementioned statement. Moreover, the hypothetical spherical structure of gaudiene, with 72-π electrons ($N = 6$), exhibits a similar behavior.[52,53]

Conclusions

In summary, the extension of the study of the magnetic response from the isotropic to an axis-specific orientation of the applied field in spherical Hirsh aromatic compounds revealed the generation of a shielding cone for three-dimensional aromatics. The study of spherical structures containing 18-, 32-, and 50-π valence electrons exhibits a similar response under specific orientations of the applied field. For these structures, the long-range character of the shielding cone was observed, in contrast to non-aromatic fullerenes, which can be informative in further NMR study of these materials. Our results expose a clear and direct connection between two- and three-dimensional aromatic structures when they are exposed to a certain orientation of the field, which may be extended to other organic and inorganic spherical aromatic structures.

Notes and references

1 F. A. Kekulé, *Bull. Soc. Chim. Biol.*, 1865, **3**, 98–110.
2 F. A. Kekulé, *Annalen der Chemie und Pharmacie*, 1866, **137**, 129–196.
3 G. Piel, *J. Chem. Educ.*, 1954, **31**, 20.
4 T. M. Krygowski, H. Szatylowicz, O. A. Stasyuk, J. Dominikowska and M. Palusiak, *Chem. Rev.*, 2014, **114**, 6383–6422.
5 T. M. Krygowski and M. K. Cyrański, *Chem. Rev.*, 2001, **101**, 1385–1420.
6 T. Heine, C. Corminboeuf and G. Seifert, *Chem. Rev.*, 2005, **105**, 3889–3910.
7 N. Martin and L. T. Scott, *Chem. Soc. Rev.*, 2015, **44**, 6397–6400.
8 G. Merino, A. Vela and T. Heine, *Chem. Rev.*, 2005, **105**, 3812–3841.
9 R. Gershoni-Poranne and A. Stanger, *Chem. Soc. Rev.*, 2015, **44**, 6597–6615.
10 R. Papadakis and H. Ottosson, *Chem. Soc. Rev.*, 2015, **44**, 6472–6493.
11 H. Miyoshi, S. Nobusue, A. Shimizu and Y. Tobe, *Chem. Soc. Rev.*, 2015, **44**, 6560–6577.
12 F. Feixas, E. Matito, J. Poater and M. Sola, *Chem. Soc. Rev.*, 2015, **44**, 6434–6451.
13 J. A. Pople, *J. Chem. Phys.*, 1956, **24**, 1111.
14 R. Islas, T. Heine and G. Merino, *Acc. Chem. Res.*, 2012, **45**, 215–228.
15 M. Kaupp, M. Bühl and V. G. Malkin, *Calculation of NMR and EPR parameters: theory and applications*, John Wiley & Sons, Inc., 2006.
16 J. A. N. F. Gomes and R. B. Mallion, *Chem. Rev.*, 2001, **101**, 1349–1384.
17 D. Sitkoff and D. A. Case, *Prog. Nucl. Magn. Reson. Spectrosc.*, 1998, **32**, 165–190.
18 D. A. Case, *Curr. Opin. Struct. Biol.*, 1998, **8**, 624–630.
19 T. Heine, C. Corminboeuf, G. Grossmann and U. Haeberlen, *Angew. Chem., Int. Ed.*, 2006, **45**, 7292–7295.
20 A. B. Sahakyan and M. Vendruscolo, *J. Phys. Chem. B*, 2013, **117**, 1989–1998.
21 J. A. Platts and K. Gkionis, *Phys. Chem. Chem. Phys.*, 2009, **11**, 10331.
22 P. Schwerdtfeger, L. N. Wirz and J. Avery, *Wiley Interdiscip. Rev.: Comput. Mol. Sci.*, 2015, **5**, 96–145.
23 V. Elser and R. C. Haddon, *Nature*, 1987, **325**, 792–794.
24 E. Osawa, H. W. Kroto, P. W. Fowler and E. Wasserman, *Philos. Trans. R. Soc., A*, 1993, **343**, 1–8.

25 M. Saunders, H. A. Jiménez-Vázquez, R. J. Cross, S. Mroczkowski, D. I. Freedberg and F. A. L. Anet, *Nature*, 1994, **367**, 256–258.
26 M. Buehl, W. Thiel, H. Jiao, P. v. R. Schleyer, M. Saunders and F. A. L. Anet, *J. Am. Chem. Soc.*, 1994, **116**, 6005–6006.
27 M. Bühl and A. Hirsch, *Chem. Rev.*, 2001, **101**, 1153–1184.
28 E. Shabtai, A. Weitz, R. C. Haddon, R. E. Hoffman, M. Rabinovitz, A. Khong, R. J. Cross, M. Saunders, P.-C. Cheng and L. T. Scott, *J. Am. Chem. Soc.*, 1998, **120**, 6389–6393.
29 Z. Chen, J. I. Wu, C. Corminboeuf, J. Bohmann, X. Lu, A. Hirsch and P. von R. Schleyer, *Phys. Chem. Chem. Phys.*, 2012, **14**, 14886.
30 D. E. Bean, J. T. Muya, P. W. Fowler, M. T. Nguyen and A. Ceulemans, *Phys. Chem. Chem. Phys.*, 2011, **13**, 20855.
31 M. P. Johansson, J. Jusélius and D. Sundholm, *Angew. Chem., Int. Ed.*, 2005, **44**, 1843–1846.
32 A. Hirsch, Z. Chen and H. Jiao, *Angew. Chem., Int. Ed.*, 2000, **39**, 3915–3917.
33 A. Muñoz-Castro, *Chem. Commun.*, 2015, **51**, 10287–10290.
34 Z. Chen and R. B. King, *Chem. Rev.*, 2005, **105**, 3613–3642.
35 Amsterdam Density Functional (ADF 2016) Code, Vrije Universiteit: Amsterdam, The Netherlands, Available at: http://www.scm.com.
36 J. P. Perdew, *Phys. Rev. B: Condens. Matter Mater. Phys.*, 1986, **33**, 8822–8824.
37 A. D. Becke, *Phys. Rev. A: At., Mol., Opt. Phys.*, 1988, **38**, 3098–3100.
38 G. Merino, T. Heine and G. Seifert, *Chem. – Eur. J.*, 2004, **10**, 4367–4371.
39 J. P. Perdew, K. Burke and Y. Wang, *Phys. Rev. B: Condens. Matter Mater. Phys.*, 1996, **54**, 16533–16539.
40 J. P. Perdew, K. Burke and M. Ernzerhof, *Phys. Rev. Lett.*, 1996, **77**, 3865–3868.
41 M. Baranac-Stojanović, *RSC Adv.*, 2014, **4**, 308–321.
42 S. Klod and E. Kleinpeter, *J. Chem. Soc. Perkin Trans. 2*, 2001, 1893–1898.
43 N. D. Charistos, A. G. Papadopoulos and M. P. Sigalas, *J. Phys. Chem. A*, 2014, **118**, 1113–1122.
44 E. Kleinpeter, S. Klod and A. Koch, *J. Org. Chem.*, 2008, **73**, 1498–1507.
45 J. Poater, M. Solà, C. Viñas and F. Teixidor, *Angew. Chem., Int. Ed.*, 2014, **53**, 12191–12195.
46 J. Aihara and H. Kanno, *THEOCHEM*, 2005, **722**, 111–115.
47 W. Wang, J. Dang and X. Zhao, *Phys. Chem. Chem. Phys.*, 2011, **13**, 14629.
48 L. Zhechkov, T. Heine and G. Seifert, *J. Phys. Chem. A*, 2004, **108**, 11733–11739.
49 X. Lu, Z. Chen, W. Thiel, P. von, R. Schleyer, R. Huang and L. Zheng, *J. Am. Chem. Soc.*, 2004, **126**, 14871–14878.
50 S.-Y. Xie, *Science*, 2004, **304**, 699.
51 A. S. Matías, R. W. A. Havenith, M. Alcamí and A. Ceulemans, *Phys. Chem. Chem. Phys.*, 2016, **18**, 11653–11660.
52 D. Sundholm, *Phys. Chem. Chem. Phys.*, 2013, **15**, 9025–9028.
53 M. Rauhalahti, A. Muñoz-Castro and D. Sundholm, *Phys. Chem. Chem. Phys.*, 2016, **18**, 18880–18886.

